Journal of Applied Polymer Science

# The Electrospun Polyamide 6 Nanofiber Membranes Used as High Efficiency Filter Materials: Filtration Potential, Thermal Treatment, and Their Continuous Production

**Yin Guibo,[1,2] Zhao Qing,[3] Zhao Yahong,[2] Yuan Yin,[2] Yang Yumin[2]**

[1]Department of Textiles, Nantong Textile Vocational Technology College, Nantong 226007, People's Republic of China
[2]Jiangsu Key Laboratory of Neuroregeneration, Nantong University, Nantong 226001, People's Republic of China
[3]Key Laboratory of People's Liberation Army, Institute of Orthopaedics, Chinese PLA General Hospital, Beijing 100853, People's Republic of China
Correspondence to: Y. Yumin (E-mail: yangym@ntu.edu.cn)

**ABSTRACT:** In this article, polyamide (PA) 6 was dissolved in 98 wt % formic acids with a concentration of 13 wt %, and then the electrospun PA 6 nanofiber membranes were prepared. The filtration potential of the nanofiber membranes were firstly analyzed based on the scanning electron microscope images and pore size measurements, and then the effects of thermal treatment on the dimensional stability were studied. Subsequently, the continuous production process based on the above experiments and the deposition areas of the nanofibers on the collecting meshes was designed. Finally, the mechanical properties and the filtration performances of the electrospun PA 6 nanofiber membranes were assessed. The results showed the membranes with a thickness of 71 $\mu$m (electrospinning for 15 min) had good filtration potential for the microparticles with 0.3 $\mu$m diameter. After being treated by tension and relaxation heat setting, the membranes demonstrated excellent dimensional stability, the breaking tenacity, and the elongation reached 4.71 $\pm$ 1.66 MPa and (69.97 $\pm$ 6.56)%, respectively. The permeability decreased with the increase of the membranes thickness. However, the permeability of membranes with (72.9 $\pm$ 1.04) $\mu$m thickness still maintained 516 L/m$^2$ s, and the actual filtration efficiency of 0.3 $\mu$m particles reached 99.98%. The above results showed that the membranes fabricated by the continuous production process could meet the demands of high efficiency filtration and provide a reference for the industrial use of electrospun nanofiber membranes. © 2012 Wiley Periodicals, Inc. J. Appl. Polym. Sci. 000: 000–000, 2012

**KEYWORDS:** PA 6; electrospinning; filtration performance; continuous production

Received 7 September 2011; accepted 16 June 2012; published online
**DOI: 10.1002/app.38211**

## INTRODUCTION

Recently, high efficiency and low resistance filters have gained much attention and have become widely used in the biomedical and industrial fields such as blood dialysis, respiratory protection, test-tube cleaning, baby ventilator hot air filtering, processing of nuclear and hazardous materials, particle collection in clean rooms, and so on.[1] In particular, fibrous filters have been widely used to separate solid matter from the particulate-laden airflow streams because of their simple structure and low cost. With respect to dirt-loading capacity, the smaller the fiber diameter used in the filters, the greater the surface area for particle absorption and the better the retention of small particles. Compared to the larger ones, small fiber diameters (in the submicron range) are well known to provide higher filtration efficiency during pressure drops and the inertial impaction stages of the filtration process.

Electrospinning is one of the simplest methods for preparing ultrafine fibers. Electrospinning is used to prepare continuous submicron to nanometer fibers. Because of their large specific surface area, high fiber aspect ratio, and high degree of interconnection, electrospun nanofibers have a variety of potential applications: as sensors, tissue engineering scaffolds, wound dressings, filters, and so on.[2] Interestingly, electrospinning can fabricate nonwoven membranes composed of nanofibers directly. These nonwoven nanofiber membranes are effective separators due to their high porosity (pore sizes ranging from tens of nanometers to several micrometers), interconnected open pore structure, high permeability, and a large surface area per unit volume.[3,4] Electrospun nanofiber membranes have now been used as air filters for over 20 years. Ki et al. prepared polyacrylonitrile (PAN) fibrous filter media with mean diameters from 270 to 400 nm by electrospinning and found that the

electrospun filters had favorable nanoparticle penetration values when compared to the commercial filters.[5] Renuga et al. dissolved polyvinylidene fluoride (PVDF) in *N,N*-dimethylacetamide (DMAc)/acetone mixture (1 : 1 vol/vol). Then they used the electrospun PVDF webs for liquid separation. They found that electrospun membranes were successful in separating more than 90% of the microparticles from the solution. This pioneering work spawned the exploration of nanofibers for more mainstream separation technology applications.[4] Additionally, Gopal et al. also prepared the electrospun polysulfone nanofiber membranes, whose bubble-point was 4.6 $\mu$m. These were able to remove above 99% of 10, 8, and 7 $\mu$m particles without any permanent fouling; and the membranes could be used as pre-filters prior to ultra- or nano-filtration.[6] Shin produced polystyrene (PS) submicron fibers from recycled expanded polystyrene (EPS) through electrospinning. These fibers were mixed with micro glass fibers to modify the filter media. They found that adding nanofibers to conventional micron-sized fibrous filter media improved the separation efficiency of the filter media from 61% to 91%.[7] Kang et al. collected poly(hexamethylene adipate) nanofibers with diameters from 80 nm to 500 nm on the electret melt-blowing nonwovens by electrospinning to form nanofiber composite membranes. They found that the filtration efficiency of this nanofiber composite membrane reached 99.9% for the particles with at least 0.3 $\mu$m diameter.[8] Feng et al. used electrospun PVDF nanofiber membranes in membrane distillation (MD) to produce drinking water (NaCl concentration $<$280 ppm) from saline water (NaCl concentration 6 wt %) by air-gap MD. They found the MD process to be competitive with conventional seawater desalination processes such as distillation and reverse osmosis.[9]

PA 6 has excellent chemical stability and thermal resistance. It is usually dissolved in formic acid from which it can be electrospun into nanofibers easily. Mit-uppatham et al. studied the influence of dependent variables such as viscosity, surface tension, and conductivity of the solution on the morphology of PA 6 fibers.[10] Pan and coworkers made an in-depth study for the performance and microstructure of electrospun PA 6 fibers.[11] Furthermore, to achieve high throughput industrial production, Pirjo and Ali designed a multi-nozzle electrospinning of PA 6 and evaluated how the different solution and process parameters affected the morphology of PA 6 fibers and production rate.[12] Aussawasathien et al. prepared the electrospun PA 6 nanofiber webs with fiber diameters from 30 nm to 110 nm, which were employed as a membrane material for water filtration because of their excellent chemical, thermal resistance, and high hydration ability. They separated 100% of the particles with sizes from 1 to 10 $\mu$m and approximately 90% of the particles with sizes about 0.5 $\mu$m. They also were able to increase the filtration efficiency and prolong the life of downstream membranes using membranes of electrospun nanofibers as pre-filters, prior to ultra- or nano-filtration.[13] Ren and Liu produced a novel sandwich structure nanofiber, a super cleaning material with a filtration efficiency as high as 99.9% for yeast.[14]

Above investigations provided the foundation for the applications of electrospun PA 6 nanofiber membranes. However, the filtration precision, permeability, and filtration efficiency of the electrospun nanofiber membranes have not been systematically studied. Meanwhile, the electrospun PA 6 nanofiber membranes exhibited poor dimensional stability and low mechanical properties, and contracted easily after immersion in water. These defects limited their filtration applications.

In this study, we first dissolved PA 6 in 98 wt % formic acids, produced electrospun nanofiber membranes with different thicknesses and preliminarily researched the filtration potential. Secondly, the effects of thermal treatment on the dimensional stability were studied and the treatment process was confirmed. Finally, according to the spraying areas of PA 6 nanofiber on the collecting meshes and the thermal treatment process, we designed the continuous production process. Subsequently, the mechanical properties and the actual filtration performances of the membranes produced by the designed process were measured. The aim of the current work is to produce electrospun PA 6 nanofiber membranes that meet the demand for high efficiency filtration and continuous production, providing a reference for the industrial use of electrospun, nanofiber membranes.

## EXPERIMENTS

### Electrospinning Conditions

PA 6 (Sigma Aldrich Inc., St. Louis, MO) was dissolved in 98 wt % formic acid (Shanghai Chemical Reagent Co., China) to prepare a 13% (w/w) spinning solution. The solutions were pumped through a syringe at a rate of 0.2 mL/h; the needle diameter was 0.9 mm. The positive charge was connected to the tip of the needle, and the negative charge attached to the metal collecting meshes.

### Morphologies of Nanofibers and Micropores

A Hitachi S-3400 scanning electron microscope (SEM) observed the morphologies of the electrospun nanofiber membranes before and after the treatment processes. The average fiber diameters were calculated by analyzing the SEM images with a custom code image analysis program (Adobe Photoshop 7.0). Pore morphologies were assessed according to the color differences generated by an image analysis program (Imagetool 3.0). The color scales ranged from 0 to 255 and were divided into three parts: the low scales stood for the micropores, namely the blank parts; the high ones are the fibers on the surface; and others are medium fiber layers. According to the bubble-point method,[4] the pore sizes were tested by a Capillary Flow Porometer (CFP-1100AI, PMI Co., USA), which could directly obtain maximum and minimum pore diameters and pore size distribution.

### Thermal Treatment

The electrospun PA 6 membranes were cut into 5 cm $\times$ 5 cm pieces, the dry heat treatment was conducted with the following process: the membranes were fixed between two pairs of rollers and then heated at 90°C for 10–20 min in an electric thermostatic drier. In contrast, the membranes were firstly wetted in demineralized water at 30°C for 10 min, secondly fixed between two pairs of rollers and finally heated at 70, 80, and 90°C for 10–20 min. Both groups of membranes were wetted again in water for 10 min and dried at room temperature to verify the

dimensional stability. The contraction rates were calculated with the following formulas:

$$\text{Contraction } (\%) = \frac{\Delta S}{S_b} \times 100 \quad (1)$$

$\Delta S$ means the size change before and after treatment, and $S_b$ stands for the size of the as-electrospun membrane.

**Mechanical Properties**

The samples produced by the continuous electrospinning process were balanced under constant temperature and humidity ($T$ = 23°C, relative humidity (RH) = 70%) for 24 h. Five points were selected in each membrane to test the thickness with a digital fabrics thickness instrument (Model YG(B)141D). The tensile test was conducted along the length of the PA 6 nanofiber membranes. They were cut into strips with a dimension of (50 × 6) mm, and then the strips were mounted on an Instron tester (Model 3365) to test the stress–strain curves at a stretching speed of 10 mm/min. The mechanical properties were characterized according to the following formulas:

$$\text{Breaking strength (MPa)} = \frac{\text{breaking force (N)}}{\text{thickness (mm)} \times \text{width (mm)}} \quad (2)$$

$$\text{Strain at break } (\%) = \left(\frac{L_1 - L_0}{L_0}\right) \times 100 \quad (3)$$

where $L_0$ is the length of sample, and $L_1$ is the length at break.

**Filtration Efficiency Evaluation**

The treated electrospun membranes were cut into circles with a diameter of 8 cm and then adhered to the polyester woven fabrics whose specifications were 50 D (warp) × 50 D (pick) × 54 × 46 (warps/cm × picks/cm). The air permeability was measured by a fabric permeability instrument (Model YG461, NingBo Textile Instrument Factory, China). Filtration efficiencies for dust particles of different diameters were evaluated by a Laser Particle Counter (Model CLG-03A, Suzhou Cleaning Technologies Research Institute, China). The flow rate was 2.83 L/min.

## RESULTS AND DISCUSSION

**Initial Filtration Potential Analysis for the Electrospun Nanofiber Membranes**

The nanofibers deposited on the mesh randomly. As a result, the thicker the membranes the more criss-crossed the nanofibers were. Criss-crossing reduces the micropore size and increases the filtration precision. In order to gauge the effects of nanofiber membrane thickness on filtration precision, the technical parameters of the electrospinning were set as follows: the spinning distance was 8 cm, the voltage was 16 kV and the feeding speed was 0.2 mL/h. Figure 1(a–c) shows the SEM images of electrospun PA 6 nanofiber membranes fabricated at different electrospinning times. It can be seen that the average fiber diameters remained unchanged as the electrospinning time increased. The electrospun PA 6 nanofibers were homogeneous, continuous, and had no beads. The average diameter was (177 ± 39) nm, and the diameter of the thinnest fiber was less than 100 nm. The electrospun nanofiber membrane provided an extremely large surface area and significantly improved filtration efficiency by absorption.

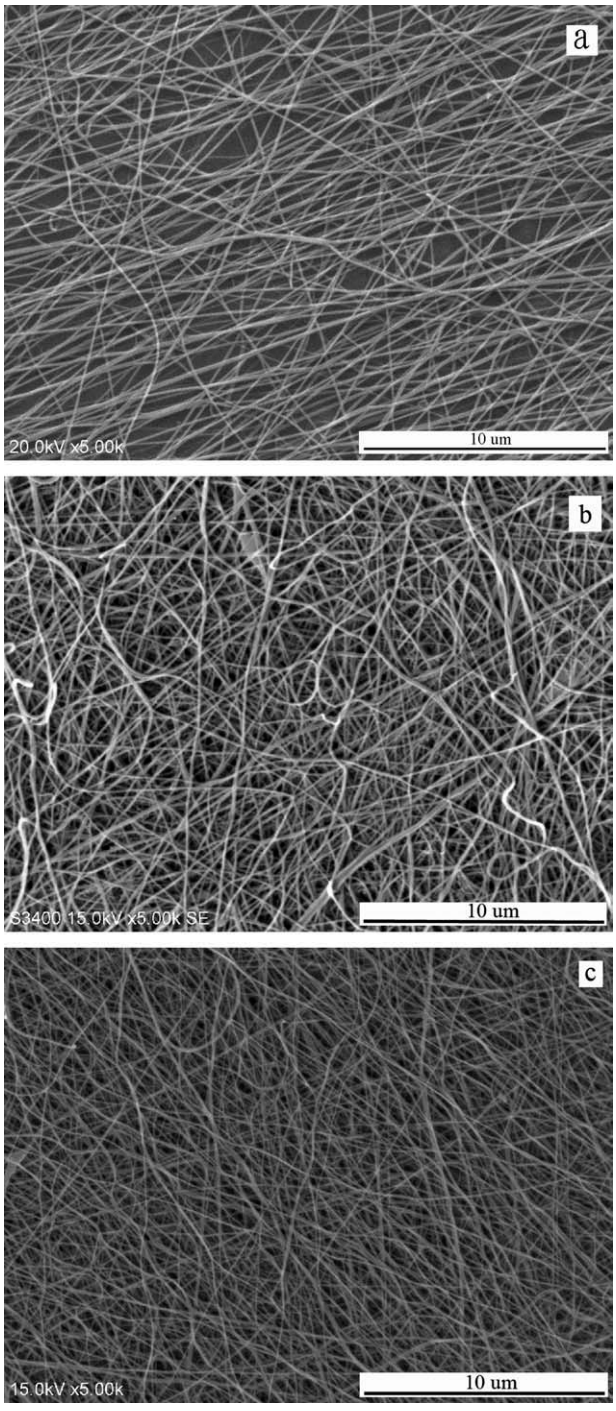


**Figure 1.** SEM images of PA 6 nanofibers membranes fabricated by electrospinning with processing times: 5 min (a), 10 min (b), and 15 min (c).

Figure 2 shows the microporous structure of PA 6 nanofiber membranes. The pore diameters are listed in Table I. As shown in Figure 2(a), only a small number of fibers accumulated after 5 min of electrospinning. The membranes demonstrated a pore size larger than 0.3 $\mu$m. Through continuous electrospinning, the thickness of nanofiber membranes increased, and they were

Applied Polymer SCIENCE

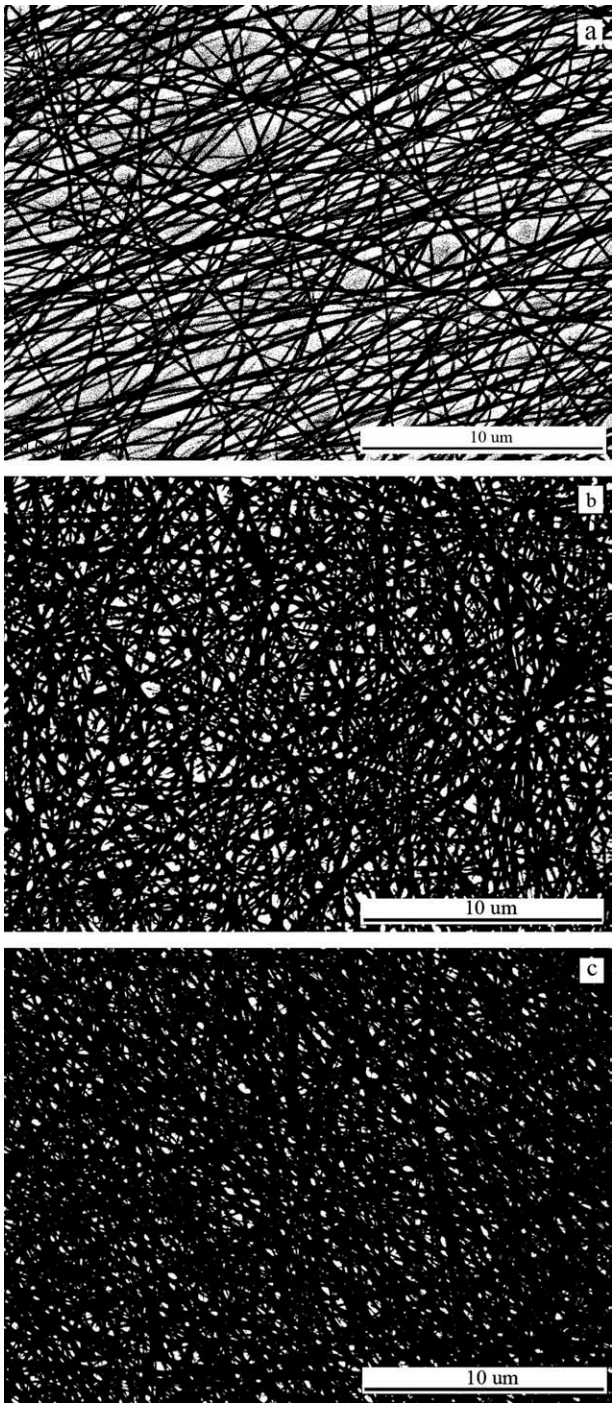


**Figure 2.** Virtual from the real SEM images of PA 6 nanofibers membranes fabricated by electrospinning with processing times: 5 min (a), 10 min (b), and 15 min (c).

similar to nonwoven fabrics. Due to the random arrangement, the nanofiber membranes demonstrated micro-porosity. Table I shows that although the electrospinning time increased from 5 min to 10 min, the thickness of the membrane did not double. Figure 2(b) shows that the pore size decreased 21.7%. Nevertheless, the maximum pore size still reached 297.9 nm. These might not filter the particles of 0.3 $\mu$m. As time passed, within 15 min of continuous electrospinning, it could be seen that the ultra-fine fiber mesh was a highly porous material filled with micro-scale interstitial spaces [Figure 2(c)]. Compared with the membranes produced by the 10 min electrospinning, the pore size decreased drastically, the maximum pore size was 212.4 nm and the average pore diameter was (147.4 $\pm$ 22.9) nm, which would completely filter the particles as small as 0.3 $\mu$m.

Although the thicker nanofiber membranes had lower pore diameters and higher filtration efficiencies for the smaller particles, permeating air had to traverse a longer distance, thus reducing air permeability, raising pressure drops, and eventually affecting filtration efficiency. Since the membranes fabricated by the 15 min electrospinning could completely satisfy the filtration requirement, the membranes with the thickness of only 71 $\mu$m produced by a 15 min electrospinning were selected and subjected to further treatment.

### Thermal Treatment of the Electrospun Nanaofiber Membranes

The electrospun nanofiber membranes usually exhibited poor dimensional stability if they were not subjected to the appropriate treatment. The contractions induced by wetting, washing, heat, and organic solvent usually made them crack. Thus a post-treatment was needed to improve their dimensional stability. As shown in Table II, the electrospun PA 6 membrane was immersed in water of less than 30°C for 10 min. Contraction reached as high as 30.67% after open air drying. When the membrane was immersed in water for 90°C for 10 min, the contraction was up to 36.27%. These tests clearly demonstrated the poor dimensional stability of the untreated membranes. Due to rapid stretching and solidification, the electrospun fibers were mostly amorphous. The pre-stress was not capable of diminishing over time, and it could induce the contractions. The heating and wetting processes could facilitate the thawing of macromolecules and eliminate pre-stress, so the effects of dry and wet heat treatment on the contraction were studied. The glass-transition temperature ($T_g$) of PA 6 is about 35–60°C, and the safe temperature range is below 90–95°C.[11] Therefore, in this experiment, we chose treatment temperatures ranging from 70 to 90°C to enhance the macromolecule movement, eliminate pre-stress, and increase dimensional stability as much as possible

**Table I.** Pore Sizes of Electrospun PA 6 Nanofiber Membranes with Different Thickness

| Electrospinning time (min) | Thickness (μm) | Max. pore size (nm) | Min. pore size (nm) | Average pore size (nm) |
|---|---|---|---|---|
| 5 | 32 ± 1.02 | 380.4 | 199.7 | 239.6 ± 49.2 |
| 10 | 58 ± 0.45 | 297.9 | 147.2 | 175.4 ± 30.6 |
| 15 | 71 ± 0.78 | 212.4 | 113.7 | 147.4 ± 22.9 |

**Table II.** Contractions of Electrospinning PA 6 Nanofibrous Membranes[a]

| | Wetting (30°C, 10 min) | Drying temperature (°C) | Drying time (min) | Contractions (%) |
|---|---|---|---|---|
| Untreated | Yes | - | - | 30.67 ± 2.28 |
| Dry heat treatment | No | 90 | 10 | 23.50 ± 3.19 |
| | No | 90 | 15 | 25.48 ± 2.98 |
| | No | 90 | 20 | 27.78 ± 1.90 |
| Water heat treatment | Yes | 90 | 10 | 14.00 ± 4.23 |
| | Yes | 90 | 15 | 12.69 ± 1.21 |
| | Yes | 90 | 20 | 15.61 ± 3.01 |
| | Yes | 70 | 15 | 17.19 ± 2.12 |
| | Yes | 80 | 15 | 15.44 ± 4.35 |

[a]The thickness of the PA 6 nanofiber membrane tested was 71 ± 0.78 μm.

It could be seen from Table II that the PA 6 nanofiber membranes were fixed and heated, then wetted and dried naturally, the contractions decreased from 30.67% to 23.50%, 25.48%, and 27.78% (corresponding to the heating time 10 min, 15 min, and 20 min, respectively). The results proved that the dry heat treatment could reduce the molecular pre-stress and enhance the dimensional stability. As opposed to the dry heat treatment, the water heat treatment could obtain a minimal contraction of 12.69%. This indicated that the combination of wetting and heat had significant inhibiting effects on the contractions of the electrospun PA 6 nanofiber membranes. During the water heat treatment, the existence of vast water molecules increased the movement ability of PA 6 macromolecules, which improved the molecular orientation and the crystallinity. The pre-stress was lessened and dimensional stability was improved.[11]

Since the combination of wetting and heat could reduce the contraction of the electrospun PA 6 nanofiber membranes, we further estimated the drying time on the contractions, the results are also shown in Table II. It could be seen that the contractions of the membranes treated by water heat treatment first decreased and then increased as the heating time increased, the minimal contraction occurred at the 15th minute. Additionally, Table II also shows that the PA 6 nanofiber membrane treated under high temperature exhibited a lower contraction. From the viewpoint of continuous and rapid production, the high temperature facilitated rapid drying and hence the drying temperature was fixed at 90°C.

In the thermal treatment experiments, because the membranes were heated under tension status (they were fixed), they did not contract during heat treatment process (whether dry heat or water heat treatment), and it just occurred in the verification procedures. That is, if they were wetted again and dried naturally, they would contract. In other words, the membrane, which was wetted, fixed, and dried only once, was just a semi-finished product and could not be used directly. In the dimensional stability experiments, we occasionally discovered that the membranes did not contract any longer if they were firstly subjected to tension water heat setting (the membranes were dried under tension status ) and then immersed in water again and dried naturally (relaxation heat setting). This illustrated that tension heat setting could relieve part of the pre-tress, but the residual pre-tress still caused contraction. Therefore, it was necessary to take other measurements of post-spinning processes to eliminate contraction completely. Thus, after tension heat treatment, the membranes underwent relaxation heat setting, making the membranes sufficiently contract without tension and attaining dimensional stability. The whole thermal treatment process was as follows: the wetted membranes were firstly fixed and dried at 90°C for 15 min (tension heat setting). Then they were wetted again and dried without tension at 90°C (relaxation heat setting). If the PA 6 nanofiber membranes fabricated using this method were again wetted and then naturally dried, the sizes would not change.

### Design of Continuous Production Process

During electrospinning, the nanofibers were collected on the metal meshes and formed a circular nanofiber membrane. While producing nanofiber membrane with certain width, the deposition area would directly influence the nozzle number and

**Table III.** Diameters of Fibers Deposition Circles at the Different Voltages and Spinning Distances

| Spinning distance (cm) | Voltage (kV) | | | | | | Average diameters (cm) | Cone angles (°) |
|---|---|---|---|---|---|---|---|---|
| | 14 | 16 | 18 | 20 | 22 | 24 | | |
| 4 | 2.6 | 2.5 | 2.2 | 2.2 | 2.1 | 2.0 | 2.27 | 31.02 |
| 6 | 3.8 | 3.6 | 3.4 | 3.1 | 3.1 | 3.1 | 3.35 | 31.12 |
| 8 | 5.6 | 5.7 | 5.8 | 5.6 | 5.4 | 5.2 | 5.55 | 37.34 |
| 10 | 8.6 | 8.5 | 8.3 | 8.3 | 7.9 | 7.5 | 8.18 | 53.28 |

Applied Polymer SCIENCE

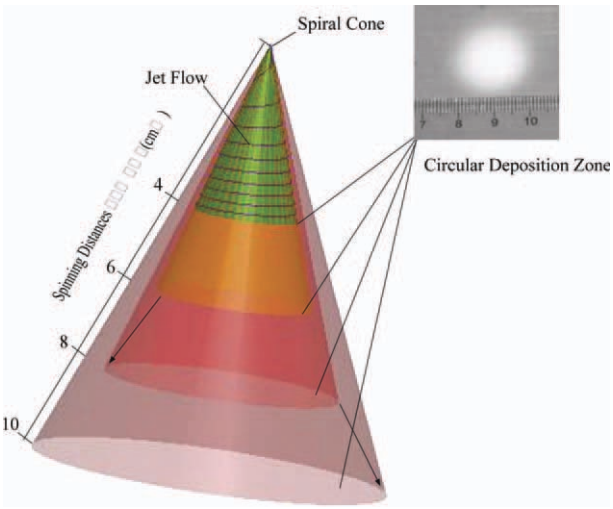


**Figure 3.** Diagram of spiral cones formed at different spinning distances. [Color figure can be viewed in the online issue, which is available at wileyonlinelibrary.com.]

production efficiency. So we first investigated the influence of voltage and distance on the nanofiber deposition areas. As shown in Table III, at the same distance, the deposition areas remained virtually unchanged with the increases of the voltage, indicating that the voltage had little effect on the deposition area. However, the distance between the nozzle and the collecting mesh significantly affected the deposition area. The farther from the nozzle to the collector, the greater was the collecting area. The mutual repulsion of the jet flow induced the formation of the spiral cone. At the same spinning distance but different voltages, according to the average diameter of the nanofiber deposition circles, we painted the diagrams of the spiral cones. As shown in Figure 3, the longer spinning distance caused the higher spraying areas. Additionally, Figure 3 and Table III both show that the spiral cone angle was about 31° at the distance of 4–6 cm. However, when the distance was raised to 8 cm, the cone angle increased to 37.12°. The cone angle further increased to 53.28° at the distance of 10 cm, which indicates that the spinning distance had obvious effects on the spraying spiral cone. With the increase of the electrospinning distance, as shown at the arrow in Figure 3, the spraying cone expanded. This phenomenon could be explained as follows. With the increase of the electrospinning distances, the electric field decreased. As a result, the spraying and splitting velocity declined; and the residence time of the jet in the spinning region prolonged. This enabled the jet flow go through the spinning zone for a longer period of time and eventually resulted in the increase in spraying area.

Though a larger spraying area could be obtained at the electrospinning distance of 10 cm, the membrane forming velocity decreased significantly. Therefore, as show in Table III, when we adopted the distance 8cm and the voltage 18 kV, the diameter of the electrospun PA 6 nanofiber deposition circle could reach 5.8 cm.

Based on the above researches, we designed an optimal continuous electrospinning and post-treatment process. As shown in Figure 4, according to the deposition area and the width of nanofiber membranes, the number of the nozzle could be calculated, the preparation process was composed of electrospinning, wetting, tension heat setting, relaxation heat setting, and coiling on the roller. In terms of this process, in this study, we adopted three nozzles and electrospun the PA 6 nanofiber membranes with the initial width of around 17 cm and the final width of 14.9 cm.

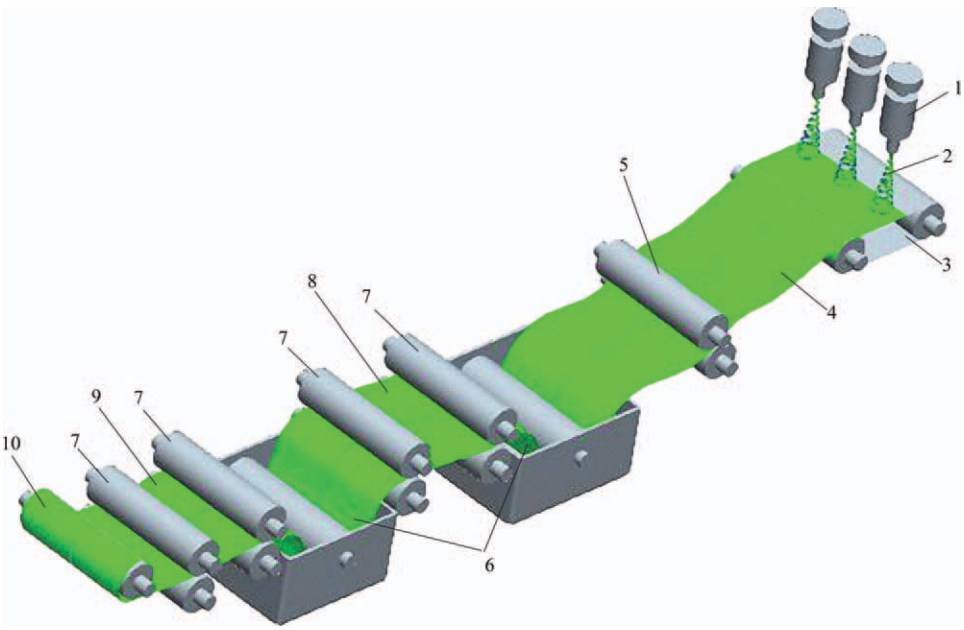


**Figure 4.** The diagram of continuous production of electrospun PA 6 nanofibrous membranes, 1—infusion pump, 2—spiral cone, 3—metallic collector, 4—electrospun nanofibrous membrane, 5—stripping rollers, 6—water bath, 7—drying rollers, 8—tension heat setting zone, 9—relaxation heat setting, 10—finished nanofiber membrane. [Color figure can be viewed in the online issue, which is available at wileyonlinelibrary.com.]

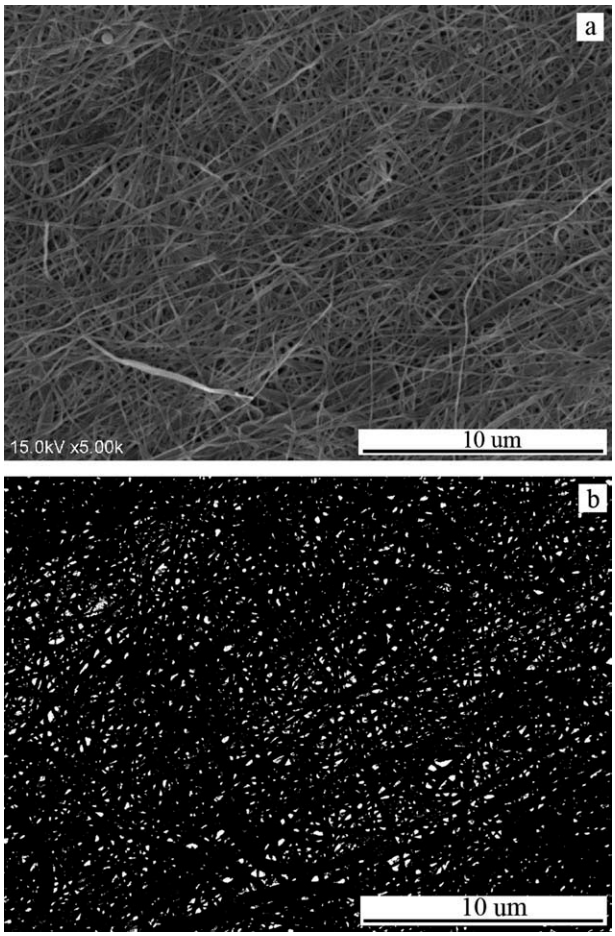


**Figure 5.** Real (a) and virtual (b) images of treated PA 6 nanofibrous membrane fabricated by electrospinning with processing time of 15 min.

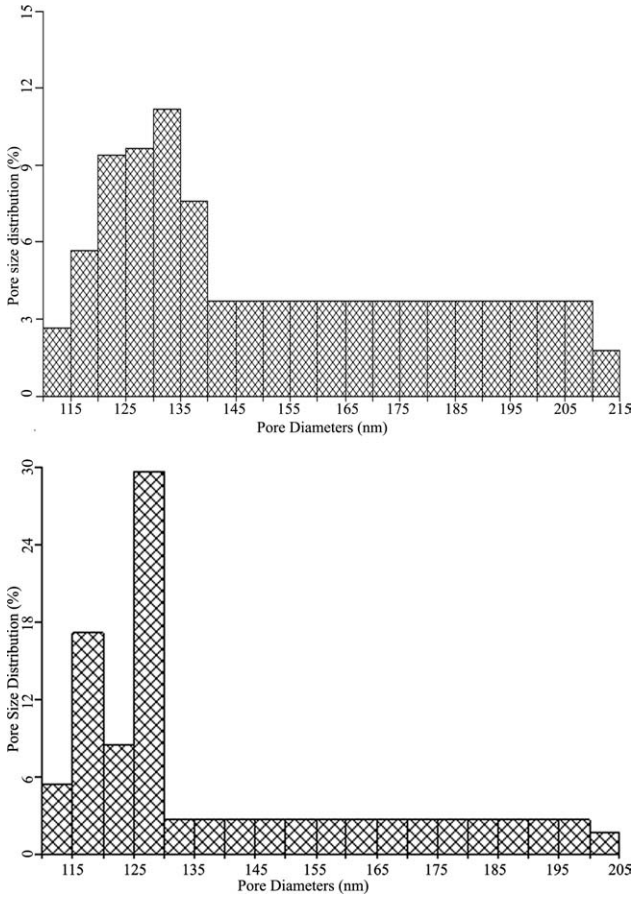


**Figure 6.** Pore size distribution of the PA 6 nanofiber membranes before (a) and after (b) treatment.

**Properties of the Finished PA 6 Nanofiber Membranes**

**Dimensional Stability and Pore Size.** In order to test the dimensional stability of the membranes obtained by the continuous production process, they were again immersed in the 30°C and 90°C water bath for 10 min, respectively. After natural drying, the results showed that the membranes exhibited excellent dimensional stability whether at the low or high temperature. This certified the feasibility of the "two-step" heat setting.

In the process of thermal treatment, the pore size might further decline due to the contraction of the nanofiber membrane; therefore, we observed the SEM images and tested their pore sizes before and after thermal treatment. Figure 5 shows the SEM images and Figure 6 shows the pore size distribution measured according to the bubble-point method. From these figures, we found that the average pore size decreased from (147.4 ± 22.9) nm to (128.6 ± 18.1) nm after thermal treatment, which would further enhance the filtration efficiency and precision.

**Mechanical Properties.** The nanofiber membranes are used as filter materials. As such, they should have the ability to endure external force. To further study the feasibility of electrospun PA 6 fibrous membranes as filter materials, we tested the mechanical properties. Figure 7 presents the stress–strain curves. It can be seen that heat treatment had significantly affected the mechanical properties of electrospun nanofiber membranes. The breaking strength of the PA 6 electrospun membrane was (1.13 ± 0.65) MPa and the elongation was (25.76 ± 4.35)%, while

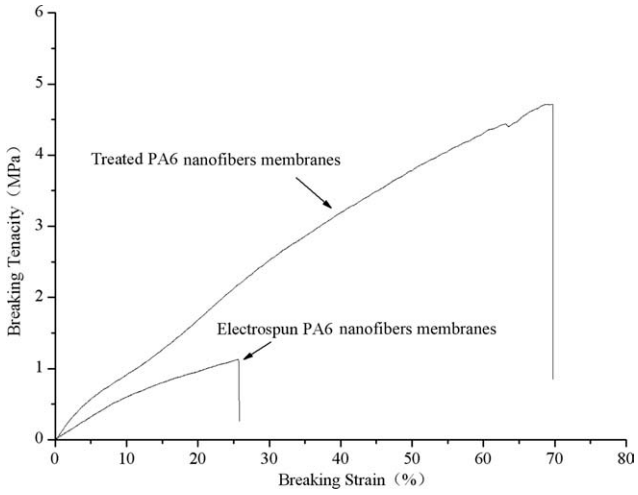


**Figure 7.** Stress–strain curves of PA 6 nanofibrous membranes before and after treatment.

**Table IV.** Air Permeability and Filtration Performances of the Treated PA 6 Nanofiber Membranes

| Samples | Membranes thickness (μm) | Areal density (g/m$^2$) | Permeability (L/m$^2$ s) | Filtration efficiency (%) Particle size (μm) | | |
|---|---|---|---|---|---|---|
| | | | | 0.3 | 0.5 | 1.0 |
| Substrate | 0 | 0 | 813 ± 119 | 0 | 0 | 9.92 ± 0.83 |
| Substrate +treated membranes[a] | 32.8 ± 0.67 | 1.21 ± 0.34 | 683 ± 143 | 81.09 ± 3.81 | 82.24 ± 2.79 | 89.78 ± 2.19 |
| | 59.2 ± 0.88 | 2.03 ± 0.28 | 581 ± 156 | 96.56 ± 0.99 | 97.91 ± 1.45 | 99.23 ± 0.31 |
| | 72.9 ± 1.04 | 2.69 ± 0.50 | 516 ± 134 | 99.98 ± 0.09 | 100 | 100 |

[a]The membranes were treated according to the process shown in Figure 4.

the breaking strength and the elongation of the electrospun PA 6 nanofiber membranes, which were produced according to the process showed in Figure 4, increased to (4.71 ± 1.66) MPa and (69.97 ± 6.56)%, respectively. The results indicate that the strength and flexibility of fiber membranes increased greatly.

**Filtration Performances.** Although the mechanical performances improved after wet heat processing, it was still difficult to meet the requirements of filter materials. So it is necessary to select appropriate fabrics (such as melt-blown fabrics, spunbond fabrics, and knitted fabrics and so on) to provide necessary support for the fragile nanofiber layer.[2] In this article, in order to eliminate the variations caused by substrates, the upper and lower micropores of the polyester fabric we selected were permeable, and their average pore diameters reached 21 μm, which was almost 100 times bigger than the pore sizes of PA 6 nanofiber membranes. Subsequently, the polyester fabric substrates had almost no effect on the filtration performance. The substrates only provided the mechanical support.

The high efficiency filter materials should not only have the ability to block the smaller particles but also have the high air permeability. Otherwise the filtration efficiency would be affected. From Table IV, it could be concluded that after the substrates were covered with nanofiber membranes, the permeability decreased dramatically. The thicker the nanofiber membranes, the lower the permeability was. The thicker the membranes, the longer the distance that the air had to traverse, which could increase the pressure drop. Moreover, the electrospun PA 6 nanofiber membrane pores contracted after treatment. The pore size of the membranes fabricated by a 15-min electrospinning would further decrease, each of which caused the permeability to fall further. However, the permeability of the treated PA 6 nanofiber membranes fabricated by a 15-min electrospinning still reached 516 L/m$^2$s, which satisfies the permeability criterion for high efficiency and low resistance filters.

As listed in Table IV, when airflow rate was 2.83 L/min, because of large-sized pores of fabric substrates, there was not any filtration effect for 0.3 μm and 0.5 μm particles, and the filtration efficiency of 1 μm particles was only 9.92%. The filtration efficiency increased after covering the substrates with PA 6 electrospun fibrous membrane whose area density was 1.21 g/m$^2$. The filtration efficiency for 1 μm, 0.5 μm, and 0.3 μm particles was 81.09%, 82.24%, and 89.78%, respectively. As area density increased to 2.03 g/m$^2$, the filtration efficiency for 1 μm particles further increased to 99.23%. When the substrates were covered with nanofiber membranes whose area density and thickness were 2.69 g/m$^2$ and 72.9 ± 1.04 μm, respectively, they were perfectly capable of trapping the particles of more than 0.5 μm in diameter. The filtration efficiency for the particles of 0.3 μm increased to 99.98%, demonstrating excellent protection against microscopic air particles. The microporous structure of electrospun nanofiber membranes generated an interception effect, which was the main reason why the nanofiber membranes had such high filtration efficiency. In addition, the fiber diameter was so small that it had larger surface energy and activity, which also improved the dirt-loading capacity. Moreover, nanofibers can carry a charge while electrospinning. Electrostatic adsorption is also likely to increase filtration efficiency.[8]

## CONCLUSIONS

In this article, we designed a continuous electrospinning and post-treatment technology. This continuous electrospinning process, especially the "two step" heat treatment process of tension and relaxation heat setting could produce PA 6 nanofiber membranes with excellent dimensional stability met the requirements for the continuous industrial production of PA 6 nanofiber membranes. The breaking strength and the elongation of the finished PA 6 membranes reached (4.71 ± 1.66) MPa and (69.97 ± 6.56)%, respectively. The filtration of the membranes with the thickness of (72.9 ± 1.04) μm and the areal density of (2.69 ± 0.50) was up to (99.98% ± 0.09)%, which also met the requirements of high efficiency filtration material. The next study is to determine the optimal process of feeding, electrospinning, wetting, drying, and coiling speed, as needed for continuous and rapid mass production.

## ACKNOWLEDGMENTS

Financial support was provided by the Natural Science Foundation of China (Grant nos. 30970713, 81171457, 30970996), the Basic Research Program of Jiangsu Province (Grant no. BK2009518), the Foundation Research Fund of Nantong (Grant no. BK2011038) and a project funded by the Priority Academic Program Development of Jiangsu Higher Education Institutions. Authors gratefully acknowledge them for their assistance.

## REFERENCES


1. Qin, X. H.; Li, N.; Yang, E. L. *Tech. Text.* **2007,** *199*, 30.
2. Qin, X. H.; Wang, S. Y. *J. Donghua Univ. (Natural SCI.)* **2007,** *1*, 15.
3. Tsai, P. P.; Schreuder-Gibson, H.; Gibson, P. *J. Electrostat.* **2002,** *54*, 333.
4. Gopal, R.; Kaur, S.; Ma, Z. W.; Chan, C.; Ramakrishna, S.; Matsuura, T. *J. Membr. Sci.* **2006,** *281*, 581.
5. Ki, M. Y.; Christopher, J.; Hogan, J.; Yasuko, M. *Chem. Eng. Sci.* **2007,** *62*, 4751.
6. Renuga, G.; Satinderpal, K.; Chao, Y. F. *J. Membr. Sci.* **2007,** *289*, 210.
7. Shin, C. *J. Colloid Interface Sci.* **2006,** *302*, 267.
8. Kang, W.; Cheng, B.; Zhuang, X. *J. Text. Res.* **2006,** *10*, 6.
9. Feng, C.; Khulbe, K. C.; Matsuura, T.; Gopal, R.; Kaur, S.; Ramakrishna, S.; Khayet, M. *J. Membr. Sci.* **2008,** *311*, 1.
10. Mit-uppatham, C.; Nithitanakul, M.; Supaphol, P. *Macromol. Chem. Phys.* **2004,** *17*, 2327.
11. Xia, Y. J.; Gao, X. Y.; Pan, Z. J. *J. Mater. Sci. Eng.* **2008,** *3*, 422.
12. Pirjo, H.; Ali, H. *Eur. Polym. J.* **2008,** *44*, 3067.
13. Aussawasathien, D.; Teerawattananon, C.; Vongachariya, A. *J. Membr. Sci.* **2008,** *315*, 11.
14. Ren, F.; Liu, T. Q. *Polym. Mater. Sci. Eng.* **2008,** *5*, 135.